# Three Dimensional Visualization for the Steam Injection into Water Pool using Electrical Resistance Tomography

Anil Kumar Khambampati [a*], Jeong Seong Lee [b], Sin Kim [b], Kyung Youn Kim[a]
[a] *Department of Electrical and Electronic Engineering, Jeju National University, Jeju 690-756*
[b] *Department of Nuclear and Energy Engineering, Jeju National University, Jeju 690-756*
[*] *Corresponding author: anil@jejunu.ac.kr*

## 1. Introduction

The direct injection of steam into a water pool is a method of heat transfer used in many process industries. The amount of research in this area however is limited to the nuclear industry, with applications relating to reactor cooling systems. Electrical resistance tomography (ERT), a low cost, non-invasive and which has high temporal resolution characteristics, can be used as a visualization tool for the resistivity distribution for the steam injection into water pool such as IRWST. In this paper, three dimensional resistivity distribution of the process is obtained through ERT using iterative Gauss-Newton method. Numerical experiments are performed by assuming different resistive objects in the water pool. Numerical results show that ERT is successful in estimating the resistivity distribution for the injection of steam in the water pool.

## 2. Electrical Resistance Tomography

In ERT, electrical current $I_l$ is injected into the object $\Omega \in \mathbb{R}^3$ through the $l$'th electrode attached on the boundary $\partial\Omega$ and the resistivity distribution $\rho$ inside the domain $\Omega$ is known, then the corresponding electrical potential $u$ in domain $\Omega$ can be determined uniquely from the Laplacian elliptic partial differential equation, which can be derived from the Maxwell equations as

$$\nabla \cdot \left( \frac{1}{\rho} \nabla u \right) = 0 \text{ in } \Omega \tag{1}$$

with the following boundary conditions based on the complete electrode model given by:

$$\int_{e_l} \frac{1}{\rho} \frac{\partial u}{\partial n} dS = I_l, \quad l = 1, 2, \cdots, L \tag{2}$$

$$\frac{1}{\rho} \frac{\partial u}{\partial n} = 0 \text{ on } \partial\Omega \setminus \bigcup_{l=1}^{L} e_l \tag{3}$$

$$u + z_l \frac{1}{\rho} \frac{\partial u}{\partial n} = \overline{U_l} \text{ on } e_l, \; l = 1, 2, \cdots, L \tag{4}$$

where $z_l$ is the effective contact impedance between $l$'th electrode, $n$ is outward unit normal, and $L$ is the total number of electrodes. Furthermore, two additional constraints for the injected currents and measured voltages are needed to ensure the existence and uniqueness of the solution:

$$\sum_{l=1}^{L} I_l = 0 \tag{5}$$

$$\sum_{l=1}^{L} \overline{U_l} = 0 \tag{6}$$

### *3.1 Forward Problem*

The resistivity distribution inside the domain has to be computed, therefore, the forward problem has to be formulated. The computation of the potential $u$ on $\Omega$ and the boundary voltages $\overline{U_l}$ on the electrodes for the given resistivity distribution and boundary conditions is called the forward problem. Finite element method (FEM) is used to obtain a numerical solution. If $u^h(x, y, z)$ is the weak solution to the problem and $\varphi_i$ are three dimensional first order piece wise linear basis functions, the potential distribution inside the domain is approximated as

$$u \approx u^h(x, y, z) = \sum_{i=1}^{N} \alpha_i \varphi_i(x, y, z) \tag{7}$$

and the potential on the electrodes is represented as

$$U^h = \sum_{j=1}^{L-1} \beta_j \mathbf{n}_j \tag{8}$$

where $N$ is the number of nodes in the finite element mesh and the bases for the measurement are $n_1 = (1, -1, 0, \cdots, 0)^T$, $n_2 = (1, 0, -1, 0, \cdots, 0)^T \in \mathbb{R}^{L \times 1}$, etc. In this $\alpha_i$ and $\beta_i$ are the nodal and boundary voltages which are to be determined. From (7) and (8), the FEM solution can be represented by linear equations

$$\mathbf{Ab} = \tilde{\mathbf{I}} \tag{9}$$

where

$$\mathbf{A} = \begin{pmatrix} \mathbf{B} & \mathbf{C} \\ C^T & \mathbf{D} \end{pmatrix}, \; \mathbf{b} = \begin{pmatrix} \boldsymbol{\alpha} \\ \boldsymbol{\beta} \end{pmatrix} \text{ and } \tilde{\mathbf{I}} = \begin{pmatrix} 0 \\ \zeta \end{pmatrix} \tag{10}$$

The detailed derivation of FEM solution can be found in [1, 2].

### *3.1 Inverse problem*

The inverse problem is to determine the internal resistivity distribution by minimizing the difference of measured and calculated voltages

$$\left\| \overline{U} - U(\rho) \right\|^2 \tag{11}$$

The regularized inverse problem can be written as

$$\left\|\bar{U}-U(\rho)\right\|^2+\alpha^2\left\|R\left(\rho-\bar{\rho}\right)\right\|^2 \quad (12)$$

where $R$ is the regularization matrix and $\alpha$ is the regularization parameter The solution to (12) gives rise to iterated Gauss-Newton equation of the form

$$\rho_{k+1}=\rho_k+\left(J^TJ+R^TR\right)^{-1}\left(J^T\left(\bar{U}-U\left(\rho_k\right)\right)\right) \quad (13)$$

here $J$ is the Jacobian $U\left(\rho\right)$ with respect to $\rho$. Jacobian is calculated based on sensitivity method. Initial guess for the resistivity distribution inside the domain is calculated using least squares as follows [1]

$$U\left(\rho_0,z_0\right)=\rho_0U\left(1,\tau\right) \quad (14)$$

where $\tau=z_0/\rho_0$ and $\rho_0$ are constants. If we set to some value and compute the best resistivity value by minimizing the cost functional

$$\left\|\bar{U}-\rho_0U\left(1,\tau\right)\right\| \quad (15)$$

The solution to the (15) can be obtain as follows

$$\rho_0=\left(U\left(1,\tau\right)^TU\left(1,\tau\right)\right)^{-1}\left(U\left(1,\tau\right)^T\bar{U}\right) \quad (16)$$

The resistivity is updated using (13) and the process is repeated until the difference between the calculated and measured voltages is minimal.

## 3. Results

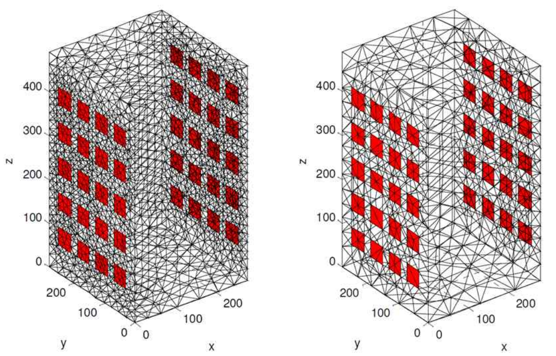

(a) (b)

Fig. 1. Finite element mesh used in synthetic data and experiment data for resistivity reconstruction. (a) fine mesh for forward solver (b) coarse mesh for inverse solver

Two different meshes (Fig. 1) are used for forward and inverse solver so that inverse crime is avoided. A fine mesh with 8473 tetrahedral elements is used to generate the voltage data. In Inverse computation, coarse mesh with 1645 tetrahedral elements is used to estimate the internal resistivity distribution. As a current injection pattern, opposite current patterns are applied. In each current injection, 10 mA is passed through the each opposite electrode pairs. A less conducting object is located inside phantom as shown in Fig. 2. Two dimensional resistivity tomograms sliced at different heights using iterated Gauss-Newton are reported. From Fig. 2, it can be noticed that the target is detected from layer 100 until 150mm with good accuracy.

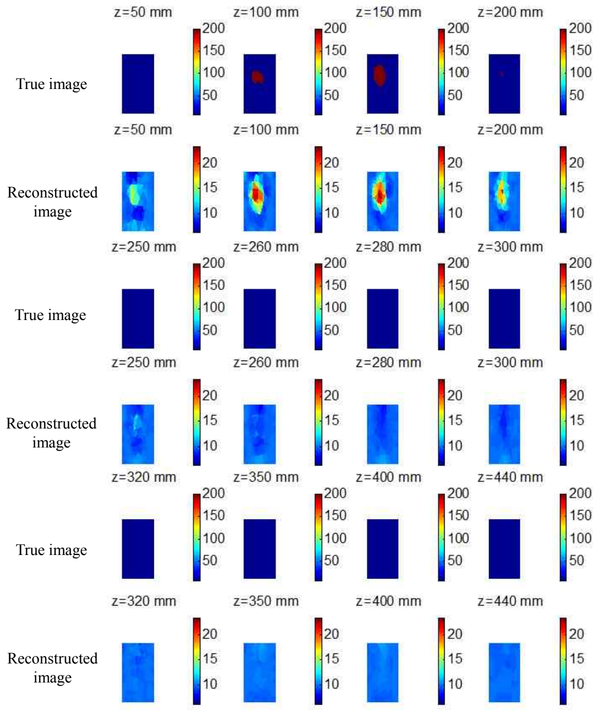


Fig. 2. Simulation result for three dimensional resistivity distribution after five iterations.

## 4. Conclusions

In this paper, we introduce a visualization technique for resistivity distribution in case of steam injection into water pool such as IWRST based on electrical resistance tomography. Electrical resistance tomography which is low cost and noninvasive method can provide three-dimensional resistivity information for the steam injection phenomena in the water pool. Resistivity distribution inside the domain is reconstructed based on finite element method and using a nonlinear inverse solver (Gauss-Newton). The numerical results show that ERT is a promising method to visualize the flow characteristics in process industries

## ACKNOWLEDGEMENTS

This research was supported by National Nuclear R&D Program through the National Research Foundation of Korea(NRF) funded by the Ministry of Education, Science and Technology (2010-0018215).

## REFERENCES

[1] P.J. Vauhkonen, M. Vauhkonen, T. Savolainen, J.P. Kaipio, Three dimensional electrical impedance tomography based on the complete electrode model, IEEE trans. Biomed. Eng., 46, pp.1150-1160, 1999.

[2] U.Z. Ijaz, B.S. Kim, T.J. Kao, A.K. Khambampati, J.S. Lee, S. Kim, K.Y. Kim, Mammography phantom studies using 3D electrical impedance tomography with numerical forward solver, In proc. Frontiers in the convergence of bioscience and information technologies, IEEE CS Press, art no 4524136, pp. 379-383, 2007.